

End-Adsorbing Tethered Polymer Layers

C. M. Wijmans

Physical Chemistry 1, Chemical Center, University of Lund,
P.O. Box 124, S-221 00 Lund, Sweden

Received June 30, 1995

Revised Manuscript Received October 23, 1995

Introduction

In this Note we consider the interaction between an end-tethered polymer layer and a solid surface which can adsorb the free end segments of the polymer chains. Our main motive for studying end-adsorbing polymer brushes is to gain a better understanding of the interaction between two surfaces in a solution containing end-adsorbing triblock copolymers. Experiments have been reported which studied both the interaction between an end-adsorbed triblock copolymer layer and a bare surface and the interaction between two such adsorbed triblock copolymer layers.¹ The equilibrium statistical thermodynamics of the interaction between two adsorbed triblock copolymer layers has been published previously.² Johner and Joanny³ have studied the interaction between a polymer brush and a bare surface which can adsorb the end segments of the polymer chains. At the equilibrium separation, they predict the volume fraction profile to contain two distinct regimes. Near the grafting surface the profile will be parabolic. Near the adsorbing surface there will be a region with constant polymer density, where no free chain ends are located ("dead zone"). This approach should be valid for relatively long chain lengths and large grafting densities. Under those conditions the noninteracting tethered polymer layer can be described using an analytic self-consistent field (SCF) theory which predicts a parabolic concentration profile. However, in experimental systems the conditions will often not be met that are required in order to have a parabolic concentration profile. We have used a more general lattice SCF model to investigate the influence of chain length and grafting density on the interaction. The predictions of this model are compared with Johner and Joanny's results. Furthermore, we briefly consider how the equilibrium interaction changes when the free end segments can also adsorb to the grafting surface.

Model

A full description of the lattice SCF model can be found in the literature. Originally developed by Scheutjens and Fleer⁴ to describe homopolymer adsorption, the theory has been extended to end-grafted chains⁵ and adsorbing copolymer chains.⁶ In this paper, we investigate the interaction between an end-tethered $B_{N-1}A_1$ polymer layer and a solid surface in a nonselective, athermal solvent. The polymer chain consists of $N - 1$ (nonadsorbing) B segments and one (adsorbing) A segment. The solution between both surfaces is divided into M parallel layers, which are numbered $z = 1, 2, 3, \dots, M$, starting in the layer adjacent to the grafting surface. Each layer consists of L lattice sites. The first B segment of each polymer chain is located in layer $z = 1$. If an A segment is in layer $z = M$, it gains an adsorption energy of $\chi_{AS}/6$ (where χ_{AS} is the Flory–Huggins parameter between A segments and surface molecules; all results presented here were computed

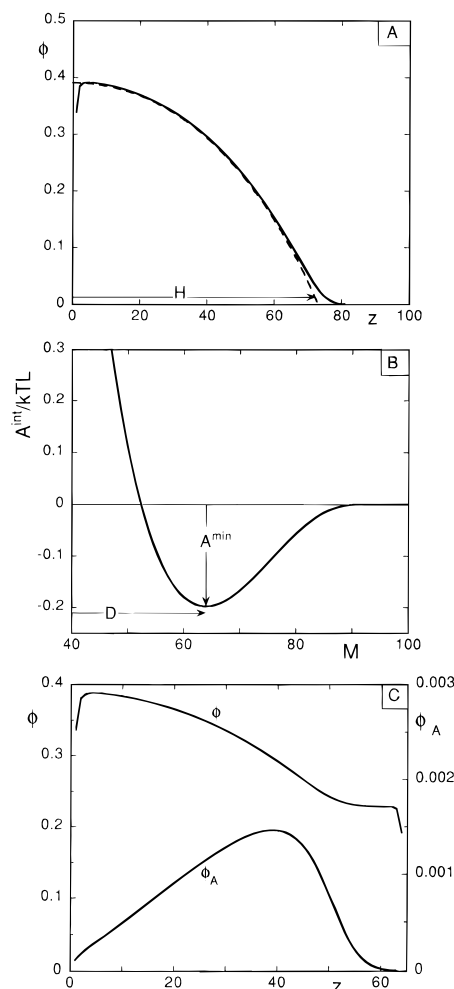


Figure 1. Volume fraction profile at large separation (A), interaction free energy curve (B), and volume fraction profiles of all segments (left ordinate) and of the adsorbing end segments only (right ordinate) for an end-adsorbing grafted polymer layer (C); $N = 200$, $\sigma = 0.1$, $\chi_{AS} = -60$. In (A), the solid curve follows from the lattice SCF theory, and the dashed curve follows from the strong-stretching approximation (see ref 5).

using a simple cubic lattice, which has a coordination number of 6).

Results and Discussion

In Figure 1A the volume fraction profile of a tethered layer is shown for $N = 200$, $\sigma = 0.1$, and $M \gg H$, so that there is no influence from the adsorbing surface. We define H as the height of the grafted layer without the exponential "foot". The value of H can be calculated using the "strong-stretching approximation". This is done in exactly the same way as described in ref 5. If the mixing free energy of a polymer brush is described using a virial expansion retaining terms up to ϕ^3 , one recovers the well-known scaling behavior $H \sim N\sigma^{1/3}$. In Figure 1B the free energy of interaction A^{int} per surface area is shown as a function of the surface separation M for $\chi_{AS} = -60$. At a certain separation D the interaction free energy has a minimum value A^{min} . The main aim of this paper is to study the dependence of this equilibrium distance D on N , σ , and χ_{AS} , as well as the structure of the polymer layer at the equilibrium separation. In Figure 1C the volume fraction profiles of the polymer (B and A segments) and of the A segments only are given for the equilibrium separation

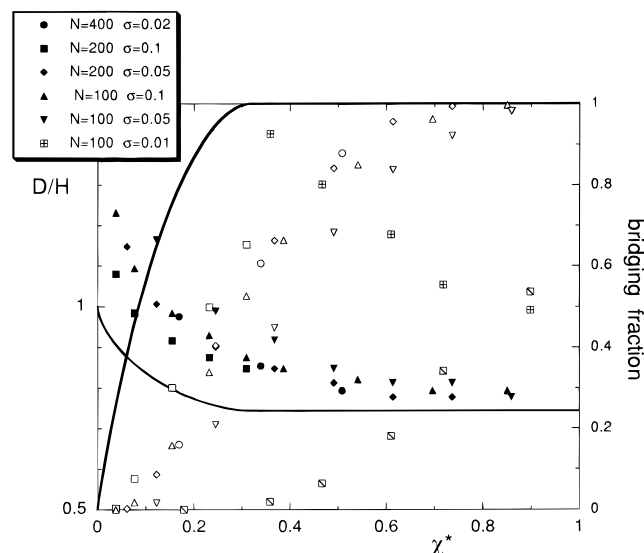


Figure 2. Equilibrium separation of the end-adsorbing tethered layer (D/H) and fraction of chains that form bridges at this separation distance as a function of the reduced adsorption strength χ^* . The values of N and σ are given in the legend. The symbols in the legend refer to D/H ; all other symbols refer to the bridging fraction. The solid curves follow from ref 3.

$M = D$. We will discuss these profiles in more detail later. In Figure 2 the results are collected for a range of different (N, σ) combinations.

The data in Figure 2 are all given as a function of the reduced adsorption parameter $\chi^* = \chi_{AS}/6N\sigma^{2/3}$ (in the "scaling picture" of a polymer brush, the free energy per chain μ is proportional to $N\sigma^{2/3}$). The open symbols in Figure 2 denote the fraction of chains that form bridges (that is, their end segment is in layer M). The filled symbols give the value of D/H .

First of all, it appears that by scaling the adsorption energy by $N\sigma^{2/3}$, most of the D/H values collapse onto a master curve with a not too large degree of scatter. However, as a general trend, the value of D/H does increase when either the grafting density is reduced at constant chain length or the chain length is decreased at constant grafting density. This increase can already clearly be seen for $(N = 100, \sigma = 0.05)$ and becomes very pronounced for $(N = 100, \sigma = 0.01)$. For these parameter sets, one moves out of the regime where the grafted layer forms a brush with a parabolic concentration profile. The chains become less strongly stretched and, what is very important in this context, the volume fraction profile is largely dominated by the exponential decay at the periphery of the grafted layer. This "foot" of the profile extends far further into the solution than the height H . That is why for $(N = 100, \sigma = 0.01)$, $D/H > 1$ over a large range of χ^* values. However, for most systems in Figure 2, $D/H > 1$ for $\chi^* < 1.5$. This indicates that at low adsorption densities the "foot" of the profile dominates the interaction even for grafting densities which are relatively high. This foot is least important for $(N = 200, \sigma = 0.1)$. For these parameters, the strong-stretching approximation works very well to describe the free (noninteracting) grafted layer (see Figure 1C).^{5,7} Nevertheless, even in this case, D/H still becomes larger than unity for low adsorption strengths. For large adsorption strengths, D/H has a limiting value of 0.8. Except for the $(N = 100, \sigma = 0.05)$ system, this limiting value is reached for $\chi^* \approx 0.6$.

The fraction of chains forming bridges shows a similar behavior as a function of χ^* as does D/H . An increase

of D/H at constant χ^* is always accompanied by a decrease of the bridging fraction. Again, for $(N = 100, \sigma = 0.05)$ the data deviate greatly from those for the other parameter sets. For large adsorption strengths, when D/H reaches its limiting value, all chains form bridges. For low adsorption strengths, the bridging fraction is zero. The range of χ^* values for which this fraction remains zero is roughly equal to that for which $D/H > 1$.

From an experimental point of view, a grafting density of 0.1 is very large for a polymer with $N = 200$. (This chain length, for example, corresponds to a molecular weight of 10^5 for polystyrene, if the diameter of one segment is taken as the length of a Kuhn segment.) A grafting density of 0.01 for a chain length of 100 segments (parameters for which χ^* must be relatively very large in order to have appreciable bridging) is still very realistic for many experimental systems.

The solid curves in Figure 2 show the predictions of Johner and Joanny for D/H and the bridging fraction (eqs 4.5, 4.11, and 4.12 in ref 3b) for an excluded volume parameter equal to unity. For a given adsorption strength, the numerical results consistently predict a lower bridging fraction and a larger value for the ratio D/H . Increasing the grafting density (or the chain length) at constant χ^* leads to a smaller D/H ratio and a larger bridging fraction. For all parameter sets, the bridging fraction becomes unity when the adsorption energy is sufficiently large. The D/H ratios from the numerical calculations are then still larger than the value of 0.744 given in ref 3.

In Figure 1C the structure of the polymer layer for $(N = 100, \sigma = 0.1, \chi_{AS} = -60)$ was given at the equilibrium separation. In this case (which corresponds to $\chi^* = 0.23$), half the chains form bridges. The volume fraction profile can indeed be divided into two distinct regimes, the polymer concentration being nearly constant over a region of 10–15 layers near the adsorbing surface. Directly adjacent to the adsorbing surface a depletion zone appears, analogous to the depletion zone at the grafting surface. The free chain end distribution has a maximum in layer 39, corresponding to the end of the parabolic zone in the strong-stretching approximation. Due to fluctuations which have to be added to the most probable distribution used in the strong-stretching approximation, the free chain end distribution does not abruptly fall off to zero beyond this maximum but decays smoothly. This causes the gradual transition from the parabolic to the constant-density regime ("dead zone") in the overall volume fraction profile. According to ref 3, the ratio of the parabolic and dead zone sizes is 0.3 for a bridging fraction equal to $1/2$.

When the polymer end groups can also adsorb to the surface onto which the chains are grafted, results different from those shown in Figure 2 can in general be expected. However, for low adsorption strengths, only relatively small deviations occur. This is illustrated in Figure 3. Here the data from Figure 2 for $(N = 100, \sigma = 0.05)$ are reproduced. Data are added for the system wherein the end segment can also adsorb to the grafting surface. For low adsorption strengths, this extra possibility to adsorb to the grafting surface has no effect on D and only a very small effect on the fraction of chains that form bridges. When the adsorption strength increases, it becomes more likely that an end segment adsorbs to the grafting surface, thus forming a loop conformation. The fraction of chains in

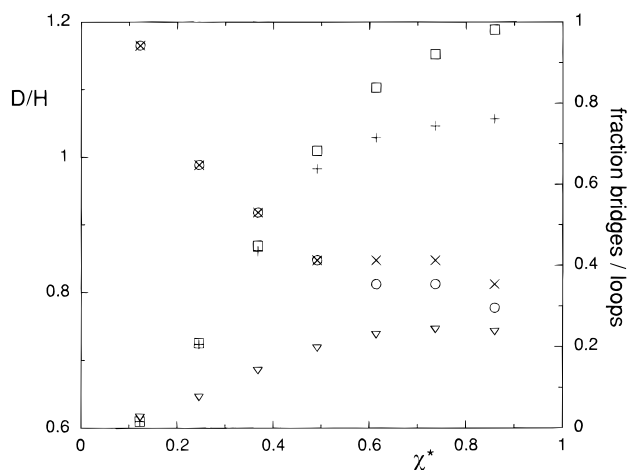


Figure 3. D/H and fraction of chains that form bridges for ($N = 100$, $\sigma = 0.05$). The circles and symbols \times give D/H for the cases that the end segments can and cannot also adsorb to the grafting surface. The squares and symbols $+$ give the bridging fraction for the cases that the end segments can and cannot also adsorb to the grafting surface. The triangles give the fraction of chains in loop conformations when the end segments can adsorb to the grafting surface.

such a loop conformation at the equilibrium separation is also shown in Figure 3. When the adsorption strength increases further, the fraction of bridging chains does not become unity, because of these loop conformations. For large adsorption strengths, D is slightly larger when the end segments can also adsorb to the grafting surface. This change in the value of D is, however, very small.

The values of χ^* in Figure 3 do not correspond to the adsorption energies of adsorbing, symmetric triblock copolymers. When $\chi^* = 3.7$, only 30% of the end segments are adsorbed to the grafting surface in the isolated tethered layer (that is, for $M \gg H$). In equilibrium, a triblock copolymer adsorbs with (a large majority of) both blocks to the surface. However, this is only the case for symmetric molecules (when both end blocks have the same adsorption energy). If one end block has a larger adsorption energy than the other, triblock copolymers will form an adsorption layer similar to the tethered layers of Figure 3. The larger the asymmetry of the polymer, the smaller χ^* will be.

Finally, we study the dependence of the interaction free energy minimum A^{\min} (see Figure 1) on N , σ , and χ^* . Johner and Joanny³ argued that the corresponding force divided by $N\sigma/H$ is a unique function of M/H , independent of N and σ . This implies that $A^{\min}/N\sigma^{5/3}$ is a unique function of χ^* . The validity of this scaling relationship is explored in Figure 4. Most of the data indeed collapse onto a master curve within a relatively small range of scatter. For ($N = 100$, $\sigma = 0.01$) the scaled free energy values are far smaller than for the

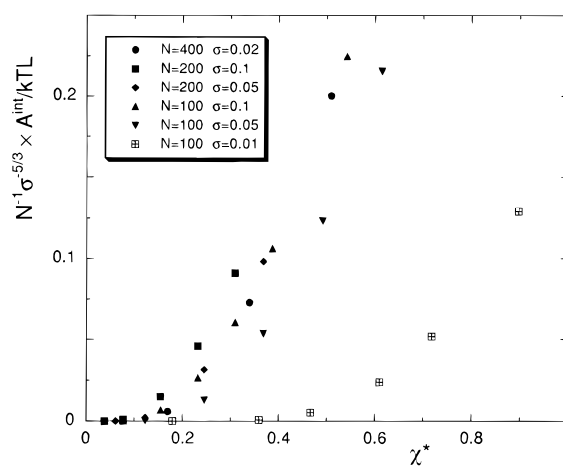


Figure 4. Scaled values of the minimum in the free energy of interaction curve as a function of χ^* . The values of N and σ are indicated in the figure.

other parameter sets. This is not surprising as for this system the fraction of chains forming bridges is also far smaller. For a given value of χ^* , the scaled free energy is always largest for ($N = 200$, $\sigma = 0.1$), as is the fraction of bridging chains. For low values of χ^* , when the fraction of bridges is (approximately) zero, the interaction free energy also approaches zero. These trends are understandable, as the attractive component of the interaction curve is due to the adsorption energy of the end segments. A practical consequence is that a small adsorbing end group added to a polymer brush will not destroy the stabilizing properties of such a system. At low grafting densities the scaled adsorption energy may even become relatively large, without a significant attraction occurring.

Acknowledgment. This work was financially supported by the Swedish Research Council for Engineering Science (TFR).

References and Notes

- (1) Dai, L.; Toprakcioglu, C. *Macromolecules* **1992**, *25*, 5495.
- (2) Dai, L.; Toprakcioglu, C.; Hadzioannou, G. *Macromolecules* **1995**, *28*, 5512.
- (3) (a) Johner, A.; Joanny, J.-F. *Europhys. Lett.* **1991**, *15*, 265.
(b) Johner, A.; Joanny, J.-F. *J. Chem. Phys.* **1992**, *96*, 6257.
- (4) Scheutjens, J. M. H. M.; Fleer, G. J. *J. Phys. Chem.* **1979**, *83*, 1619. Scheutjens, J. M. H. M.; Fleer, G. J. *Macromolecules* **1985**, *18*, 1882.
- (5) Wijmans, C. M.; Scheutjens, J. M. H. M.; Zhulina, E. B. *Macromolecules* **1992**, *25*, 2567.
- (6) Evers, O. A.; Scheutjens, J. M. H. M.; Fleer, G. J. *Macromolecules* **1990**, *23*, 5221.
- (7) Milner, S. T. *J. Chem. Soc., Faraday Trans.* **1990**, *86*, 1349.

MA9509319